

cis-Dihydroxylation of Alkenes with Oxone Catalyzed by Iron Complexes of a Macrocyclic Tetraaza Ligand and Reaction Mechanism by ESI-MS Spectrometry and DFT Calculations

Toby Wai-Shan Chow, Ella Lai-Ming Wong, Zhen Guo, Yungen Liu,
Jie-Sheng Huang, and Chi-Ming Che*

Department of Chemistry and Open Laboratory of Chemical Biology of the Institute of Molecular Technology for Drug Discovery and Synthesis, The University of Hong Kong, Pokfulam Road, Hong Kong

Received February 3, 2010; E-mail: cmche@hku.hk

Abstract: $[\text{Fe}^{\text{III}}(\text{L-N}_4\text{Me}_2)\text{Cl}_2]^+$ (**1**, L-N₄Me₂ = *N,N'*-dimethyl-2,11-diaza[3.3](2,6)pyridinophane) is an active catalyst for *cis*-dihydroxylation of various types of alkenes with oxone at room temperature using limiting amounts of alkene substrates. In the presence of 0.7 or 3.5 mol % of **1**, reactions of electron-rich alkenes, including cyclooctene, styrenes, and linear alkenes, with oxone (2 equiv) for 5 min resulted in up to >99% substrate conversion and afforded *cis*-diol products in up to 67% yield, with *cis*-diol/epoxide molar ratio of up to 16.8:1. For electron-deficient alkenes including α,β -unsaturated esters and α,β -unsaturated ketones, their reactions with oxone (2 equiv) catalyzed by **1** (3.5 mol %) for 5 min afforded *cis*-diols in up to 99% yield with up to >99% substrate conversion. A large-scale *cis*-dihydroxylation of methyl cinnamate (9.7 g) with oxone (1 equiv) afforded the *cis*-diol product (8.4 g) in 84% yield with 85% substrate conversion. After catalysis, the L-N₄Me₂ ligand released due to demetalation can be reused to react with newly added $\text{Fe}(\text{ClO}_4)_2 \cdot 4\text{H}_2\text{O}$ to generate an iron catalyst *in situ*, which could be used to restart the catalytic alkene *cis*-dihydroxylation. Mechanistic studies by ESI-MS, isotope labeling studies, and DFT calculations on the **1**-catalyzed *cis*-dihydroxylation of dimethyl fumarate with oxone reveal possible involvement of *cis*-HO-Fe^V=O and/or *cis*-O=Fe^V=O species in the reaction; the *cis*-dihydroxylation reactions involving *cis*-HO-Fe^V=O and *cis*-O=Fe^V=O species both proceed by a concerted but highly asynchronous mechanism, with that involving *cis*-HO-Fe^V=O being more favorable due to a smaller activation barrier.

Introduction

Metal-catalyzed *cis*-dihydroxylation of alkenes is an important method for C–O bond formation reactions in organic synthesis, as elegantly demonstrated by tremendous studies on such *cis*-dihydroxylation reactions catalyzed by OsO₄,¹ particularly the Sharpless asymmetric dihydroxylation protocol, which has wide applications^{1b–h} and can be performed on large scales.² A number of OsO₄-catalyzed large-scale *cis*-dihydroxylation reactions using *N*-methylmorpholine *N*-oxide (NMO) as terminal oxidant have also been known.² Since OsO₄ is highly toxic and

osmium compounds are expensive, there is an increasing interest in developing *cis*-dihydroxylation catalysts of other transition metals such as ruthenium,^{3–5} manganese,^{6,7} and iron,^{8–12} of which only ruthenium^{2b,5} and manganese^{7a} catalysts have been

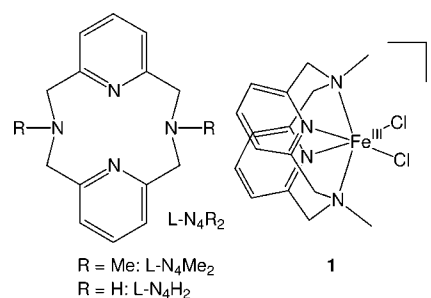
- (1) (a) Schröder, M. *Chem. Rev.* **1980**, *80*, 187. (b) Kolb, H. C.; Van Nieuwenhze, M. S.; Sharpless, K. B. *Chem. Rev.* **1994**, *94*, 2483. (c) Gao, Y. In *Encyclopedia of Reagents for Organic Synthesis*; Paquette, L. A., Ed.; Wiley: New York, 1995; Vol. 6, p 3801. (d) Johnson, R. A.; Sharpless, K. B. In *Catalytic Asymmetric Synthesis*, 2nd ed.; Ojima, I., Ed.; Wiley-VCH: New York, 2000; p 357. (e) Bolm, C.; Hildebrand, J. P.; Muñoz, K. In *Catalytic Asymmetric Synthesis*, 2nd ed.; Ojima, I., Ed.; Wiley-VCH: New York, 2000; p 399. (f) Kolb, H. C.; Sharpless, K. B. In *Transition Metals for Organic Synthesis*; Beller, M.; Bolm, C., Eds.; Wiley-VCH: Weinheim, Germany, 2004; Vol. 2, p 275. (g) Zaitsev, A. B.; Adolffson, H. *Synthesis* **2006**, 1725. (h) Salvador, J. A. R.; Silvestre, S. M.; Moreira, V. M. *Curr. Org. Chem.* **2008**, *12*, 492.
- (2) (a) *Catalysts for Fine Chemical Synthesis*; Roberts, S. M., Poignant, G., Eds.; John Wiley & Sons, Ltd.: New York, 2002; Vol. 1 (Hydrolysis, Oxidation and Reduction), p 105. (b) Caron, S.; Dugger, R. W.; Ruggeri, S. G.; Ragan, J. A.; Ripin, D. H. B. *Chem. Rev.* **2006**, *106*, 2943.
- (3) (a) Shing, T. K. M.; Tai, V. W.-F.; Tam, E. K. W. *Angew. Chem., Int. Ed. Engl.* **1994**, *33*, 2312. (b) Shing, T. K. M.; Tam, E. K. W.; Tai, V. W.-F.; Chung, I. H. F.; Jiang, Q. *Chem.–Eur. J.* **1996**, *2*, 50. (c) Shing, T. K. M.; Tam, E. K. W. *Tetrahedron Lett.* **1999**, *40*, 2179.
- (4) (a) Plietker, B.; Niggemann, M. *Org. Lett.* **2003**, *5*, 3353. (b) Plietker, B.; Niggemann, M.; Pollrich, A. *Org. Biomol. Chem.* **2004**, *2*, 1116. (c) Plietker, B.; Niggemann, M. *Org. Biomol. Chem.* **2004**, *2*, 2403. (d) Plietker, B.; Niggemann, M. *J. Org. Chem.* **2005**, *70*, 2402. (e) Plietker, B. *Synthesis* **2005**, 2453.
- (5) (a) Ho, C.-M.; Yu, W.-Y.; Che, C.-M. *Angew. Chem., Int. Ed.* **2004**, *43*, 3303. (b) Yip, W.-P.; Ho, C.-M.; Zhu, N.; Lau, T.-C.; Che, C.-M. *Chem.–Asian J.* **2008**, *3*, 70.
- (6) De Vos, D. E.; de Wildeman, S.; Sels, B. F.; Grobet, P. J.; Jacobs, P. A. *Angew. Chem., Int. Ed.* **1999**, *38*, 980.
- (7) (a) Brinkma, J.; Schmieder, L.; van Vliet, G.; Boaron, R.; Hage, R.; De Vos, D. E.; Alsters, P. L.; Feringa, B. L. *Tetrahedron Lett.* **2002**, *43*, 2619. (b) de Boer, J. W.; Brinkma, J.; Browne, W. R.; Meetsma, A.; Alsters, P. L.; Hage, R.; Feringa, B. L. *J. Am. Chem. Soc.* **2005**, *127*, 7990.
- (8) (a) Chen, K.; Que, L., Jr. *Angew. Chem., Int. Ed.* **1999**, *38*, 2227. (b) Costas, M.; Tipton, A. K.; Chen, K.; Jo, D.-H.; Que, L., Jr. *J. Am. Chem. Soc.* **2001**, *123*, 6722. (c) Ryu, J. Y.; Kim, J.; Costas, M.; Chen, K.; Nam, W.; Que, L., Jr. *Chem. Commun.* **2002**, 1288. (d) Fujita, M.; Costas, M.; Que, L., Jr. *J. Am. Chem. Soc.* **2003**, *125*, 9912. (e) Oldenburg, P. D.; Shteinman, A. A.; Que, L., Jr. *J. Am. Chem. Soc.* **2005**, *127*, 15672. (f) Suzuki, K.; Oldenburg, P. D.; Que, L., Jr. *Angew. Chem., Int. Ed.* **2008**, *47*, 1887.

applied to *cis*-dihydroxylation of alkenes on >1 g scale. In view of the inexpensiveness and biocompatibility of iron, the development of practical iron catalysts for alkene *cis*-dihydroxylation would be of high interest.

cis-Dihydroxylation of alkenes catalyzed by iron complexes was pioneered by Que and co-workers.⁸ Over the past decade, a series of iron-catalyzed alkene *cis*-dihydroxylation reactions using H₂O₂ as terminal oxidant,^{8–12} along with in-depth mechanistic studies,^{13–16} have been reported, predominantly by Que and co-workers, mainly to develop functional models for nonheme iron enzymes Rieske dioxygenases.^{17,18} These iron-catalyzed reactions display the following features: (i) excess alkene substrates were used, (ii) significant amounts of epoxides were formed as byproducts, (iii) the reactions were performed on small scales, and (iv) no recycling of catalysts was studied. Exceptions to feature (ii) are the high *cis*-diol selectivities, obtained using excess alkene substrates (with H₂O₂ as terminal oxidant), in the *cis*-dihydroxylation of electron-deficient alkenes reported by Que and co-workers^{8d,f} and in the *cis*-dihydroxylation of cyclooctene reported by Costas and co-workers.¹¹ Notably, as an exception to feature (i), the *cis*-dihydroxylation reactions of electron-rich aliphatic alkenes (such as oct-1-ene and hept-2-ene) and cyclohexene reported by Que and co-workers^{8c} were performed using limiting amounts of alkene substrates, with *cis*-diol/epoxide ratios of (1.5–4.3):1; this is hitherto the sole report on iron-catalyzed *cis*-dihydroxylation in which alkene substrates were used in limiting amounts. It remains a formidable challenge to realize iron-catalyzed *cis*-dihydroxylation of alkenes that not only uses limiting amounts of alkene substrates but also has high *cis*-diol selectivity and is applicable to large-scale synthesis.

Our interest in iron-catalyzed *cis*-dihydroxylation of alkenes was initiated on the basis of our previous works on this type of organic transformations mediated/catalyzed by ruthenium

Chart 1



complexes.^{5,19} We have demonstrated that *cis*-dioxoruthenium(VI) complexes react with alkenes to afford *cis*-diols through a [3 + 2] cycloaddition mechanism,¹⁹ which suggests that other reactive *cis*-dioxometal complexes, including those of naturally abundant metals such as iron, could also undergo *cis*-dihydroxylation of alkenes with a similar mechanism. We therefore endeavored to explore the possibility of extending the oxidation chemistry of *cis*-dioxometal complexes from ruthenium to iron. Among our hypotheses is the potential utility of alkene *cis*-dihydroxylation by *cis*-dioxoiron(V) species. Previously we have isolated and structurally characterized a *cis*-dioxoruthenium(V) complex bearing a tetradentate tertiary amine ligand,²⁰ this, along with earlier reports on bent [O=Fe^V=O]⁺ (O–Fe–O angle: ~85°) generated in gas phase and characterized by mass spectrometry and theoretical calculations,²¹ lends credence to the possible existence of *cis*-dioxoiron(V) species in solution. A strategy is to use macrocyclic tertiary amine ligands to support *cis*-dioxoiron units, similar to the use of such auxiliary ligands in the reactive *cis*-dioxoruthenium complex [(Me₃tacn)(CF₃-CO₂)Ru^{VI}O₂]ClO₄ (Me₃tacn = *N,N,N'*-trimethyl-1,4,7-triazacyclononane)¹⁹ and in the catalyst [Ru^{III}(Me₃tacn)Cl₃]; the latter can catalyze *cis*-dihydroxylation of alkenes with H₂O₂ on 100 g scale.^{5b} However, we found that changing the ruthenium of [Ru^{III}(Me₃tacn)Cl₃] to iron rendered the complex ineffective in catalyzing alkene *cis*-dihydroxylation with H₂O₂.

During our quest for practical iron catalysts for *cis*-dihydroxylation of alkenes, we came across a highly efficient *cis*-dihydroxylation of electron-deficient alkenes by oxone (potassium peroxydisulfate, 2KHSO₅·KHSO₄·K₂SO₄)²² catalyzed by an iron(III) complex, [Fe^{III}(L-N₄Me₂)Cl₂]⁺ (**1**, L-N₄Me₂ = *N,N'*-dimethyl-2,11-diaza[3.3](2,6)pyridinophane, Chart 1), which bears a macrocyclic tetraaza ligand L-N₄Me₂²³ containing both tertiary amine and pyridyl units. This iron complex, together with its catecholate analogues containing the same L-N₄Me₂ ligand, was first reported by Krüger and co-workers.²⁴ The use, in this work, of oxone—an inexpensive, commercially available, and environmentally benign oxidant—was inspired by previous

- (9) Klopstra, M.; Roelfes, G.; Hage, R.; Kellogg, R. M.; Feringa, B. L. *Eur. J. Inorg. Chem.* **2004**, 846.
- (10) Bruijninx, P. C. A.; Buurmans, I. L. C.; Gosiewska, S.; Moelands, M. A. H.; Lutz, M.; Spek, A. L.; van Koten, G.; Klein Gebbink, R. J. M. *Chem.—Eur. J.* **2008**, *14*, 1228.
- (11) Company, A.; Gómez, L.; Fontrodona, X.; Ribas, X.; Costas, M. *Chem.—Eur. J.* **2008**, *14*, 5727.
- (12) Barry, S. M.; Rutledge, P. J. *Synlett* **2008**, *14*, 2172.
- (13) (a) Chen, K.; Costas, M.; Kim, J.; Tipton, A. K.; Que, L., Jr. *J. Am. Chem. Soc.* **2002**, *124*, 3026. (b) Mairata i Payeras, A.; Ho, R. Y. N.; Fujita, M.; Que, L., Jr. *Chem.—Eur. J.* **2004**, *10*, 4944. (c) Mas-Ballesté, R.; Fujita, M.; Hemmila, C.; Que, L., Jr. *J. Mol. Catal. A: Chem.* **2006**, *251*, 49. (d) Mas-Ballesté, R.; Costas, M.; van den Berg, T.; Que, L., Jr. *Chem.—Eur. J.* **2006**, *12*, 7489. (e) Mas-Ballesté, R.; Que, L., Jr. *J. Am. Chem. Soc.* **2007**, *129*, 15964.
- (14) Bukowski, M. R.; Comba, P.; Lienke, A.; Limberg, C.; Lopez de Laorden, C.; Mas-Ballesté, R.; Merz, M.; Que, L., Jr. *Angew. Chem., Int. Ed.* **2006**, *45*, 3446.
- (15) Bautz, J.; Comba, P.; Lopez de Laorden, C.; Menzel, M.; Rajaraman, G. *Angew. Chem., Int. Ed.* **2007**, *46*, 8067.
- (16) (a) Bassan, A.; Blomberg, M. R. A.; Siegbahn, P. E. M.; Que, L., Jr. *J. Am. Chem. Soc.* **2002**, *124*, 11056. (b) Quiñero, D.; Musaev, D. G.; Morokuma, K. *Inorg. Chem.* **2003**, *42*, 8449. (c) Bassan, A.; Blomberg, M. R. A.; Siegbahn, P. E. M. *J. Biol. Inorg. Chem.* **2004**, *9*, 439. (d) Bassan, A.; Blomberg, M. R. A.; Siegbahn, P. E. M.; Que, L., Jr. *Angew. Chem., Int. Ed.* **2005**, *44*, 2939. (e) Quiñero, D.; Morokuma, K.; Musaev, D. G.; Mas-Ballesté, R.; Que, L., Jr. *J. Am. Chem. Soc.* **2005**, *127*, 6548. (f) Comba, P.; Rajaraman, G. *Inorg. Chem.* **2008**, *47*, 78.
- (17) For reviews, see: (a) Rohde, J.-U.; Bukowski, M. R.; Que, L., Jr. *Curr. Opin. Chem. Biol.* **2003**, *7*, 674. (b) Oldenburg, P. D.; Que, L., Jr. *Catal. Today* **2006**, *117*, 15. (c) Shan, X.; Que, L., Jr. *J. Inorg. Biochem.* **2006**, *100*, 421. (d) Que, L., Jr.; Tolman, W. B. *Nature* **2008**, *455*, 333. (e) Bruijninx, P. C. A.; van Koten, G.; Klein Gebbink, R. J. M. *Chem. Soc. Rev.* **2008**, *37*, 2716.
- (18) Feng, Y.; Ke, C.-y.; Xue, G.; Que, L., Jr. *Chem. Commun.* **2009**, 50.

- (19) Yip, W.-P.; Yu, W.-Y.; Zhu, N.; Che, C.-M. *J. Am. Chem. Soc.* **2005**, *127*, 14239.
- (20) Li, C.-K.; Che, C.-M.; Tong, W.-F.; Tang, W.-T.; Wong, K.-Y.; Lai, T.-F. *J. Chem. Soc., Dalton Trans.* **1992**, 2109.
- (21) Schröder, D.; Fiedler, A.; Schwarz, J.; Schwarz, H. *Inorg. Chem.* **1994**, *33*, 5094.
- (22) *The Chemistry of Peroxides*; Rappoport, Z., Ed.; John Wiley & Sons, Ltd.: Chichester, U.K., 2006; Vol. 2.
- (23) Bottino, F.; Grazia, M. D.; Finocchiaro, P.; Fronczek, F. R.; Mamo, A.; Pappalardo, S. *J. Org. Chem.* **1988**, *53*, 3521.
- (24) (a) Koch, W. O.; Krüger, H.-J. *Angew. Chem., Int. Ed. Engl.* **1995**, *34*, 2671. (b) Koch, W. O.; Schünemann, V.; Gerdan, M.; Trautwein, A. X.; Krüger, H.-J. *Chem.—Eur. J.* **1998**, *4*, 686. (c) Koch, W. O.; Schünemann, V.; Gerdan, M.; Trautwein, A. X.; Krüger, H.-J. *Chem.—Eur. J.* **1998**, *4*, 1255.

works of Yang,²⁵ Shi,²⁶ and co-workers on ketone-catalyzed oxidation using oxone as a terminal oxidant.

Herein is reported the **1**-catalyzed *cis*-dihydroxylation of a variety of alkenes, particularly electron-deficient ones, by oxone with high *cis*-diol selectivity. These highly selective reactions are striking in several aspects: (i) The alkene substrates were used in limiting amounts. (ii) *cis*-Diol products could be prepared on ~10 g scale. (iii) Replacing oxone with H₂O₂ rendered the *cis*-dihydroxylation ineffective, in contrast to the general use of H₂O₂ in previously reported iron-^{8–12} and ruthenium-catalyzed^{5b} *cis*-dihydroxylation of alkenes. (iv) Oxone is an ineffective oxidant in the alkene *cis*-dihydroxylation using ruthenium catalysts,⁵ and, to the best of our knowledge, no efficient *cis*-dihydroxylation of alkenes with oxone catalyzed by a metal complex has been reported in literature. Also reported here are mechanistic studies on the **1**-catalyzed alkene *cis*-dihydroxylation reactions by means of electrospray ionization mass spectrometry (ESI-MS) and DFT calculations.

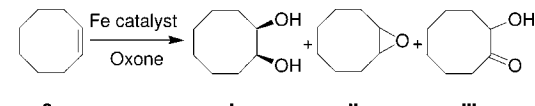
Results and Discussion

Catalyst Screening. Iron complexes of macrocyclic tetraaza ligands L-N₄R₂ (Chart 1), including [Fe^{III}(L-N₄Me₂)(cat)]⁺ (cat = catecholate ligands) reported by Krüger and co-workers²⁴ and [Fe^{III}(L-N₄H₂)Cl₂]⁺ reported by Girerd, Banse, and co-workers,²⁷ were previously studied as model systems for catechol dioxygenases (which catalyze oxidative cleavage of C–C bonds of catechols with molecular oxygen).^{24,27} In this work, we screened complexes [Fe^{III}(L-N₄Me₂)Cl₂]⁺ (**1**) and [Fe^{III}(L-N₄H₂)Cl₂]⁺, together with [Fe^{III}(Me₃tacn)Cl₃], [Fe^{II}(ppy)Cl₂] (ppy = 2,2':6',2'':6'',2''':6''',2''''-quinquepyridine), and [Fe^{II}(6-Me₂-bpmcn)-Cl₂] (6-Me₂-bpmcn = *N,N'*-dimethyl-*N,N'*-bis(6-methyl-2-pyridylmethyl)-*trans*-1,2-diaminocyclohexane), for their catalytic properties toward alkene *cis*-dihydroxylation. Both FeCl₄[−] and ClO₄[−] salts of **1** were used; the crystal structures of **1**•FeCl₄[−] and **1**•ClO₄[−]•MeCN have been determined by X-ray crystallography (see Table S1 and Figures S1 and S2 in the Supporting Information), which have Fe–N_{py} distances of 2.116(2)–2.1288(16) Å and Fe–N_{amine} distances of 2.219(2)–2.237(2) Å similar to those of **1** previously reported by Krüger and co-workers (Fe–N_{py} 2.130 Å, Fe–N_{amine} 2.232 Å).^{24b}

At the outset, we examined the reaction of cyclooctene (**2a**) with oxone (2 equiv) at room temperature using [Fe^{III}(Me₃tacn)-Cl₃] (3.5 mol %) as catalyst, in view of the catalytic activity of [Ru^{III}(Me₃tacn)Cl₃] for alkene *cis*-dihydroxylation.^{5b} After 5 min, the [Fe^{III}(Me₃tacn)Cl₃]-catalyzed reaction gave a 55% substrate conversion but afforded *cis*-diol product **I** in only 3% yield, and the major product is epoxide **II**, which was formed in 27% yield based on consumed substrate (entry 1, Table 1). When the catalyst was changed to [Fe^{II}(ppy)Cl₂], [Fe^{II}(6-Me₂-bpmcn)-Cl₂], or [Fe^{III}(L-N₄H₂)Cl₂]⁺, no *cis*-diol **I** was detected in the reaction mixtures (entries 2–4, Table 1).

Interestingly, replacing the NH group (in the L-N₄H₂ ligand) of [Fe^{III}(L-N₄H₂)Cl₂]⁺ with NMe group to form [Fe^{III}(L-N₄Me₂)Cl₂]⁺ (**1**) endowed the catalyst with a good activity toward *cis*-dihydroxylation of cyclooctene with oxone, probably due to enhanced stability of **1** toward oxidative deterioration, as L-N₄Me₂, unlike L-N₄H₂, does not bear secondary amine NH

Table 1. Oxidation of Cyclooctene (**2a**) with Oxone Using Various Iron Catalysts^a



entry	catalyst	conv (%) ^b	yield (%) based on conv			I/II	mass balance (%)
			I ^c	II ^c	III ^c		
1	[Fe ^{III} (Me ₃ tacn)Cl ₃]	55	3	27	<i>d</i>	0.1:1	30
2	[Fe ^{II} (ppy)Cl ₂]	42	<i>d</i>	58	<i>d</i>		58
3	[Fe ^{II} (6-Me ₂ -bpmcn)Cl ₂]	0	<i>d</i>	<i>d</i>	<i>d</i>		
4	[Fe ^{III} (L-N ₄ H ₂)Cl ₂] ⁺	38	<i>d</i>	30	3		33
5	[Fe ^{III} (L-N ₄ Me ₂)Cl ₂] ⁺ (1)	99	53	8	12	6.6:1	73
6	[Fe ^{III} (L-N ₄ Me ₂)Br ₂] ⁺	96	45	4	12	11.3:1	61
7 ^e	[Fe ^{III} (L-N ₄ Me ₂)Cl ₂] ⁺ (1)	96	60 ^f	5	12	12:1	77
8 ^g	[Fe ^{III} (L-N ₄ Me ₂)Cl ₂] ⁺ (1)	37	<i>d</i>	34	9		44

^a Reaction conditions: cyclooctene (0.5 mmol), catalyst (3.5 mol %) in MeCN (6 mL), oxone (2 equiv) and NaHCO₃ (6 equiv) in H₂O (6 mL) added in 2 portions, RT, 5 min. ^b Determined by ¹H NMR. ^c Determined by GC. ^d Not detected in the reaction mixture. ^e Catalyst loading: 0.7 mol %. ^f Isolated yield. ^g H₂O₂ (35% aq, 6 equiv), instead of oxone, was used, added in 3 portions within 90 min.

groups susceptible to oxidation by oxone.²⁸ The FeCl₄[−] and ClO₄[−] salts of **1** displayed similar catalytic activities toward this reaction. Control experiments using [Et₄N][FeCl₄] (3.5 mol %) as catalyst resulted in only ~16% substrate conversion, and no *cis*-diol **I** was detected in the reaction mixture; the corresponding epoxide **II** was formed in ~6% yield based on the starting substrate. As the preparation of the FeCl₄[−] salt of **1** is more convenient, this salt of **1** was used in subsequent catalytic studies.

The **1**-catalyzed *cis*-dihydroxylation of cyclooctene with oxone at room temperature resulted in a 99% substrate conversion within 5 min, and the *cis*-diol **I** was formed as the major product in 53% yield (based on the consumed substrate) whereas epoxide **II** in 8% yield, giving a **I**/**II** ratio of 6.6:1 (entry 5, Table 1). A higher **I**/**II** ratio of 11.3:1 was obtained using [Fe^{III}(L-N₄Me₂)Br₂]⁺ (FeBr₄[−] salt) as catalyst, but this catalyst gave *cis*-diol **I** in a lower yield of 45% (entry 6, Table 1). The mass balance obtained using catalyst **1** is 73% (entry 5, Table 1), substantially higher than those (30–61%) obtained using the other iron catalysts (entries 1, 2, 4, 6; Table 1). No *cis*-diol was detected in the reaction mixture when the reaction was performed in the absence of **1** under the same conditions.

Decreasing the loading of **1** from 3.5 mol % to 0.7 mol % resulted in a slight increase of mass balance, with the *cis*-diol selectivity (**I**/**II** ratio) increasing from 6.6:1 to 12:1 (cf entries 5, 7; Table 1). By changing the terminal oxidant to H₂O₂, the reaction (loading of **1**: 3.5 mol %) afforded epoxide in 34% yield (entry 8, Table 1); no *cis*-diol **I** was detected in the reaction mixture. Regardless whether oxone or H₂O₂ was used as terminal oxidant, α-hydroxy ketone **III** was formed as a minor product (12% and 9% yields, respectively) in the **1**-catalyzed oxidation of cyclooctene (entries 5, 8; Table 1).

We next studied the reaction of methyl cinnamate (**3a**) with oxone (2 equiv) at room temperature in the presence of catalyst **1** at different loadings (Table 2). Remarkably, using 3.5 mol % of **1**, the reaction afforded *cis*-diol product **I** in 81% yield with 98% substrate conversion within 5 min, together with trace amounts of epoxide **II**, α-hydroxy ketone **III**, and benzaldehyde

(25) Yang, D. *Acc. Chem. Res.* **2004**, *37*, 497.

(26) (a) Shi, Y. *Acc. Chem. Res.* **2004**, *37*, 488. (b) Wong, O. A.; Shi, Y. *Chem. Rev.* **2008**, *108*, 3958.

(27) Raffard, N.; Carina, R.; Simaan, A. J.; Sainton, J.; Rivière, E.; Tchertanov, L.; Bourcier, S.; Bouchoux, G.; Delroisse, M.; Banse, F.; Girerd, J.-J. *Eur. J. Inorg. Chem.* **2001**, 2249.

(28) Gella, C.; Ferrer, E.; Alibés, R.; Busqué, F.; de March, P.; Figueredo, M.; Font, J. J. *Org. Chem.* **2009**, *74*, 6365.

Table 2. *cis*-Dihydroxylation of Methyl Cinnamate (**3a**) with Oxone Catalyzed by **1** at Different Catalyst Loadings^a

entry	catalyst loading (%)	conv (%)	yield (%) based on conv				I/II	mass balance (%)
			I ^b	II ^c	III ^b	IV ^c		
1	3.5	98	81	4	4	2	20.3:1	91
2	1.4	94	84	5	<i>d</i>	3	16.8:1	92
3	0.7	49	86	6	<i>d</i>	1	14.3:1	93
4	0.35	52	85	10	<i>d</i>	4	8.5:1	99
5	0	0	<i>d</i>	<i>d</i>	<i>d</i>	<i>d</i>		

^a Reaction conditions: substrate (0.5 mmol), **1** (0–3.5 mol %) in MeCN (6 mL), oxone (2 equiv) and NaHCO₃ (6 equiv) in H₂O (6 mL) added in 2 portions, RT, 5 min. ^b Determined by ¹H NMR. ^c Determined by GC. ^d Not detected in the reaction mixture.

IV, with a high *cis*-diol selectivity (**I/II**) of 20.3:1 and mass balance of 91% (entry 1, Table 2). The *cis*-diol selectivity and substrate conversion decreased, although the mass balance increased, with decreasing loading of catalyst **1** (entries 1–4, Table 2). At catalyst loadings of 0.35–1.4 mol %, no α -hydroxy ketone **III** was detected in the reaction mixture (entries 2–4, Table 2).

Substrate Scope. The **1**-catalyzed *cis*-dihydroxylation of alkenes with oxone (2 equiv) at room temperature could be applicable to a variety of alkene substrates, from electron-rich ones including cyclic alkene (**2a**), aryl alkenes (**2b–e**), and linear alkenes (**2f–h**), to electron-deficient ones including α,β -unsaturated esters (**3a,f–j**) and α,β -unsaturated ketones (**3b–e**) (Table 3).

For the electron-rich alkenes, the highest yields of *cis*-diols **I** and highest substrate conversion and mass balances were obtained for terminal aryl alkenes **2b,d**, which were converted to *cis*-diols **I** in 65–67% yields with >99% substrate conversion within 5 min, giving the **I/II** ratios of up to 16.8:1 and mass balances of 95–100% (entries 2, 4; Table 3). In the *cis*-dihydroxylation of **2a–e**, α -hydroxy ketones **III** were formed in 8–23% yields (entries 1–5, Table 3), and, for **2b–e**, aldehydes **IV** were also formed (in 5–9% yields). Notably, byproducts **II–IV** were not detected in the reaction mixtures for the oxidation of linear terminal alkenes **2f,g** (entries 6, 7; Table 3); these two alkenes were converted to *cis*-diols **I** in 64% and 53% yields, respectively, with moderate substrate conversions (52–71%) and mass balances (53–64%).

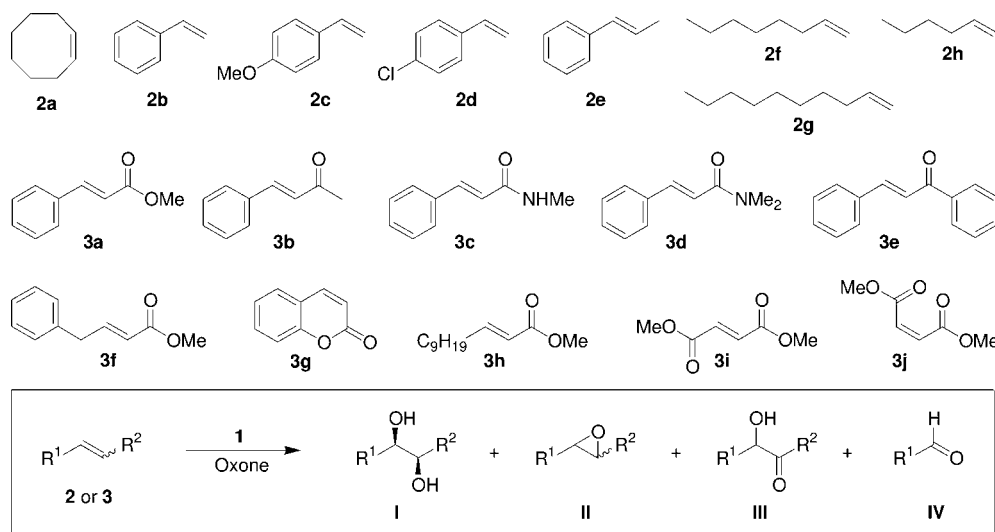
Electron-deficient alkenes **3a–j**, except **3h**, were generally converted into *cis*-diols **I** with good-to-excellent values of *cis*-diol yields (60–99%), substrate conversions (84 to >99%), and mass balances (60–99%) (entries 9–15, 17, 18; Table 3) and high **I/II** ratios ((8.5–20.3):1, entries 9–13 in Table 3). No α -hydroxy ketones **III** were detected in the reaction mixtures, except for **3a**; epoxides **II** and aldehydes **IV** were formed in only up to 8% yield or in about half the cases not detectable. Strikingly, the **1**-catalyzed oxidation of dimethyl fumarate (**3i**) with oxone at room temperature for 5 min produced no detectable amounts of byproducts **II–IV** and afforded *cis*-diol **I** in 99% yield with >99% substrate conversion and 99% mass balance (entry 17, Table 3).

Overoxidation Issue. Owing to the use of limiting amounts of substrates, overoxidation could occur in the presence of excess oxidant; however, this was not found to be a serious problem in the **1**-catalyzed oxidation of alkenes with oxone (2 equiv) at room temperature, at least for the alkene substrates giving good-to-excellent mass balances as depicted in Table 3. The byproducts

α -hydroxy ketones **III** formed in the *cis*-dihydroxylation of **2a–e** and **3a** (Table 3) could be due to overoxidation and/or a direct ketohydroxylation of these alkenes. We treated *cis*-diol **I** (obtained from *cis*-dihydroxylation of cyclooctene) with oxone (2 equiv) in the presence of **1** (0.7 mol %) at room temperature for 5 min; this reaction afforded the corresponding **III** in 23% yield with 68% substrate conversion (Scheme S1 in Supporting Information). We also examined the mass flow during the *cis*-dihydroxylation of cyclooctene with oxone (2 equiv) catalyzed by **1** (3.5 mol %), and found that the mass balance, and the yield of *cis*-diol **I** as well, markedly decreased with increasing reaction time (Figure S3 in the Supporting Information). Provided that such loss in mass balance is mainly due to overoxidation, the corresponding overoxidation should largely give other unidentified products, as the yield of **III** was little changed with reaction time.

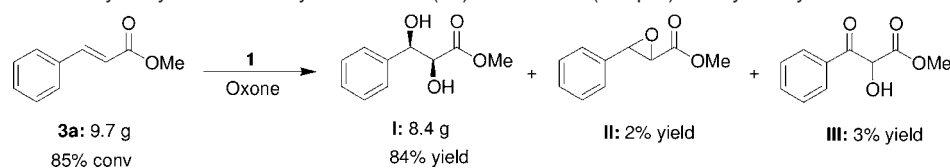
While **1** can catalyze alkene *cis*-dihydroxylation with oxone using limiting amounts of alkene substrates, higher product turnover numbers (TON) could be obtained by using excess amounts of alkenes, partly due to minimization of overoxidation. For the *cis*-dihydroxylation of cyclooctene (**2a**) catalyzed by **1** (0.7 mol %), the TON of *cis*-diol product **I** increased from 82 to 158 upon changing substrate/oxidant ratio from 1:2 to 5:1 (entries 1, 2; Table S2 in the Supporting Information); α -hydroxy ketone **III** was still formed, but the ratio of **III/I** decreased from 1:5.1 to 1:8.8. An increase in product TON, upon changing substrate/oxidant ratio from 1:2 to 5:1, was also observed for the *cis*-dihydroxylation of **2e,h** and **3g** (entries 3–8, Table S2 in the Supporting Information).

Large-Scale Reactions. We explored the feasibility of scaling up the **1**-catalyzed *cis*-dihydroxylation to ~10 g scale. A one-pot reaction of 9.7 g of methyl cinnamate (**3a**) with oxone (1 equiv) in the presence of **1** at room temperature for 10 min gave 8.4 g of *cis*-diol **I** (84% yield, 85% substrate conversion, Scheme 1). This large-scale reaction was performed by adding each of the substrate and catalyst in two equal portions with each portion reacting for 5 min (see Experimental Section); interestingly, in adding the second portion of catalyst, Fe(ClO₄)₂·4H₂O was used, without the need to use complex **1**. A control experiment revealed that Fe(ClO₄)₂·4H₂O alone is not an active catalyst for the alkene *cis*-dihydroxylation. We speculate that at the end of the **1**-catalyzed oxidation of **3a** with oxone, the ligand L-N₄Me₂ was released due to demetalation, and the *cis*-dihydroxylation of **3a** could also be catalyzed by an iron complex generated in situ from reaction of L-N₄Me₂ with Fe(ClO₄)₂·4H₂O. If such is the case, multiple reuse of L-N₄Me₂ for complexation with new batch of Fe(ClO₄)₂·4H₂O in the catalysis could be feasible.

Table 3. *cis*-Dihydroxylation of Alkenes (**2a–h** and **3a–j**) with Oxone Catalyzed by **1**^a

entry	substrate	conv (%) ^b	yield (%) based on conv				I/II	mass balance (%)
			I ^c	II ^b	III ^d	IV ^{b,d}		
1	2a	96	60	5	12	<i>e</i>	12:1	77
2	2b	>99	67	4	17 ^c	7	16.8:1	95
3	2c	>99	46	<i>e</i>	23 ^c	9		78
4	2d	>99	65	9	18 ^c	8	7.2:1	100
5	2e	89	44	19	8	5	2.3:1	76
6	2f	71	64	<i>e</i>	<i>e</i>	<i>e</i>		64
7	2g	52	53	<i>e</i>	<i>e</i>	<i>e</i>		53
8	2h	97	16 (36 ^f)	2	<i>e</i>	<i>e</i>	8:1	18
9	3a	94	81	4	4	2	20.3:1	91
10	3b	92	65	6	<i>e</i>	8	10.8:1	79
11	3c	90	73	5	<i>e</i>	2	14.6:1	80
12	3d	90	72	6	<i>e</i>	2	12:1	80
13	3e	>99	68 (75 ^f)	8	<i>e</i>	2	8.5:1	78
14	3f	84	61	<i>e</i>	<i>e</i>	2		63
15	3g	94	60 (67 ^f)	<i>e</i>	<i>e</i>	<i>e</i>		60
16	3h	34	56 (65 ^f)	<i>e</i>	<i>e</i>	<i>e</i>		56
17	3i	>99	99	<i>e</i>	<i>e</i>	<i>e</i>		99
18	3j	94	77	<i>e</i>	<i>e</i>	<i>e</i>		77

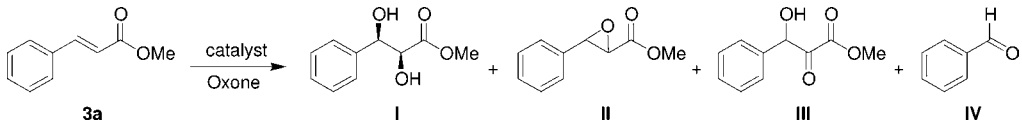
^a Reaction conditions: substrate (0.5 mmol), **1** (0.7 mol % for entries 1, 5, 8, 15; 3.5 mol % for the other entries) in MeCN (6 mL), oxone (2 equiv) and NaHCO₃ (6 equiv) in H₂O (6 mL) added in 2 portions, RT, 5 min. ^b Determined by GC. ^c Isolated yield. ^d Determined by ¹H NMR. ^e Not detected in the reaction mixture. ^f Yield determined by ¹H NMR.

Scheme 1. Large-Scale *cis*-Dihydroxylation of Methyl Cinnamate (**3a**) with Oxone (2 equiv) Catalyzed by **1**^a

^a Benzaldehyde (**IV**) was formed in <1% yield.

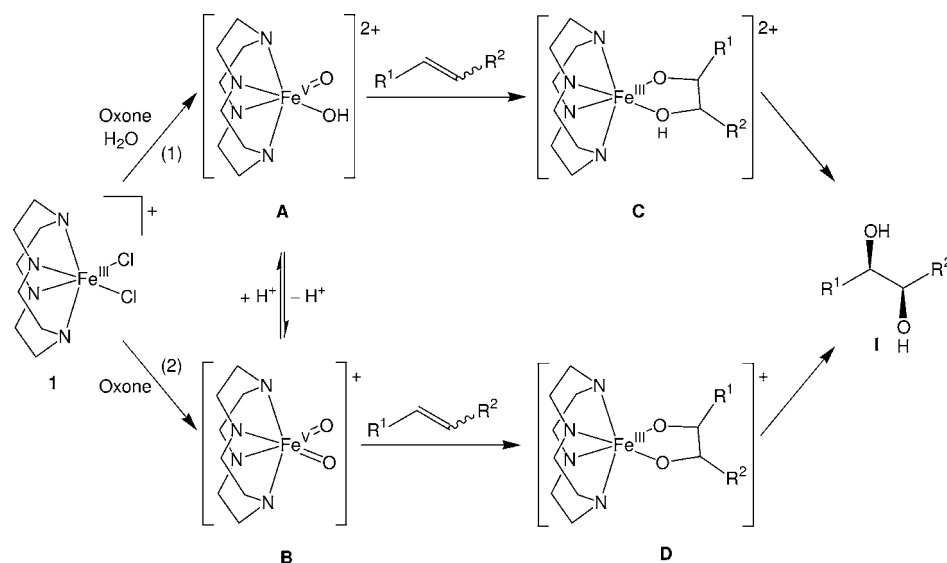
Reuse of L-N₄Me₂ Ligand. Before focusing on the reuse of L-N₄Me₂, we examined the reactions of cyclooctene (**2a**) and methyl cinnamate (**3a**) with oxone (2 equiv) at room temperature using a 1:1 mixture of Fe(ClO₄)₂·4H₂O and L-N₄Me₂ as catalyst at different catalyst loadings (0.35–3.5 or 0.7–3.5 mol %). These reactions indeed mainly converted both **2a** and **3a** to the corresponding *cis*-diol **I** products, with 53–96% substrate conversions, 54–63% *cis*-diol yields, (4.2–9.2):1 **I/II** ratios, and 71–82% mass balances for **2a**, and 56–96% substrate conversions, 78–86% *cis*-diol yields, (21.5–28.7):1 **I/II** ratios, and 82–94% mass balances for **3a** (Table S3 in the Supporting Information), demonstrating a similar catalytic activity of “Fe(ClO₄)₂·4H₂O + L-N₄Me₂” to that of **1**.

Given the highest *cis*-diol selectivity (**I/II** ratio: 28.7:1), coupled with excellent substrate conversion and mass balance, in the *cis*-dihydroxylation of **3a** with oxone (2 equiv) at a catalyst loading of 1.4 mol % (entry 5, Table S3 in the Supporting Information), we studied the reuse of L-N₄Me₂ for the same reaction at this catalyst loading. The first run was carried out using catalyst **1**; in subsequent runs, the catalyst was generated in situ by direct reaction of added Fe(ClO₄)₂·4H₂O with the L-N₄Me₂ released during previous run (no isolation of the released L-N₄Me₂ was required). Upon reusing L-N₄Me₂ five times, the reaction still gave good overall substrate conversion of 85% and *cis*-diol yield of 89% (entry 3, Table 4). This demonstrates that the macrocyclic tetraaza

Table 4. Reuse of L-N₄Me₂ in *cis*-Dihydroxylation of Methyl Cinnamate (**3a**) with Oxone Catalyzed by **1** or "Fe(ClO₄)₂·4H₂O + L-N₄Me₂"^a


entry	times reused	accumulated conv (%) ^b	accumulated yield (%) based on conv				I/II	mass balance (%)
			I ^b	II ^c	III ^b	IV ^c		
1	1	98	84	5	<i>d</i>	3	16.8:1	92
2	3	95	84	9	3	1	9.3:1	100
3	5	85	89	<i>d</i>	3	3		98

^a Reaction conditions for the 1st run: methyl cinnamate (0.5 mmol), **1** (1.4 mol %) in MeCN (6 mL), oxone (2 equiv) and NaHCO₃ (6 equiv) in H₂O (6 mL) added in 2 portions, RT, 5 min; reaction conditions for the other runs: methyl cinnamate (0.5 mmol) and Fe(ClO₄)₂·4H₂O (1.4 mol %) in MeCN (6 mL), oxone (2 equiv) and NaHCO₃ (6 equiv) in H₂O (6 mL) added in 2 portions, RT, 5 min. ^b Determined by ¹H NMR. ^c Determined by GC. ^d Not detected in the reaction mixture.

Scheme 2. Possible Pathways of **1**-Catalyzed *cis*-Dihydroxylation of Alkenes with Oxone

ligand L-N₄Me₂ is robust toward the *cis*-dihydroxylation of alkenes with oxone.

Mechanistic Aspects. Depending on the ligands in the iron catalysts, iron-catalyzed *cis*-dihydroxylation of alkenes with H₂O₂ is documented to involve several types of active intermediates, including *cis*-HO-Fe^V=O and Fe^{III}-(η²-OOH) intermediates in water-assisted (wa) and nonwater-assisted (nwa) mechanisms, respectively, established by Que and co-workers,^{17b} together with a *cis*-Fe^{IV}(OH)₂ intermediate recently proposed by Comba and co-workers.¹⁵ Similar species could also be considered as candidates for the active intermediate in the **1**-catalyzed alkene *cis*-dihydroxylation with oxone. Another candidate is the iron analogue of the *cis*-dioxoruthenium complexes that are reactive toward *cis*-dihydroxylation of alkenes as described in our previous work.¹⁹

In literature, oxone is known to show various oxidation behaviors and can undergo heterolytic and homolytic O–O bond cleavage to effect two-²⁹ and one-electron³⁰ oxidation of metal ions, respectively. In most of its reactions with trivalent metal

ions, oxone is proposed to act as a single oxygen atom donor by undergoing heterolytic O–O bond cleavage,²⁹ resulting in two-electron oxidation of metal ions, examples of which include the generation of HO-M^V=O (M = Fe^{29c} and Mn^{29b,d}) intermediates, previously proposed by Meunier,^{29b,c} Groves,^{29d} and co-workers, from reaction of iron(III) or manganese(III) porphyrins with oxone in aqueous solutions at pH 7–8, with the second oxygen atom coming from H₂O.^{29b,c} Similar generation of [Fe^V(L-N₄Me₂)(O)(OH)]²⁺ (*cis*-HO-Fe^V=O species **A**, Scheme 2) from treatment of the iron(III) complex **1** with oxone in MeCN/H₂O (1:1 v/v) under the catalytic conditions (pH 7) was proposed in this work (reaction 1 in Scheme 2) as one of the possible mechanisms. Another mechanism we proposed here is the reaction of **1** with more than one equivalent of oxone to generate [Fe^V(L-N₄Me₂)O₂]⁺ (*cis*-O=Fe^V=O species **B**, Scheme 2) with its oxygen atoms both coming from oxone (reaction 2 in Scheme 2); however, this mechanism could be complex, which might involve homolytic O–O bond cleavage. The *cis*-HO-Fe^V=O species **A** could be in equilibrium with the *cis*-O=Fe^V=O species **B** through deprotonation and protonation, respectively, analogous to a HO-Mn^V=O porphyrin species in equilibrium with an O=Mn^V=O porphyrin species in solution as reported by Groves and co-workers.³¹ Intermediates **A** and **B** could also be generated in the catalytic reactions using "Fe(ClO₄)₂·4H₂O + L-N₄Me₂" via initial one-electron oxidation

(29) For examples, see: (a) Labat, G.; Meunier, B. *J. Org. Chem.* **1989**, *54*, 5008. (b) Pitié, M.; Bernadou, J.; Meunier, B. *J. Am. Chem. Soc.* **1995**, *117*, 2935. (c) Sorokin, A.; Meunier, B. *Eur. J. Inorg. Chem.* **1998**, 1269. (d) Jin, N.; Groves, J. T. *J. Am. Chem. Soc.* **1999**, *121*, 2923.

(30) Lente, G.; Kalmár, J.; Baranyai, Z.; Kun, A.; Kék, I.; Bajusz, D.; Takács, M.; Veres, L.; Fábián, I. *Inorg. Chem.* **2009**, *48*, 1763.

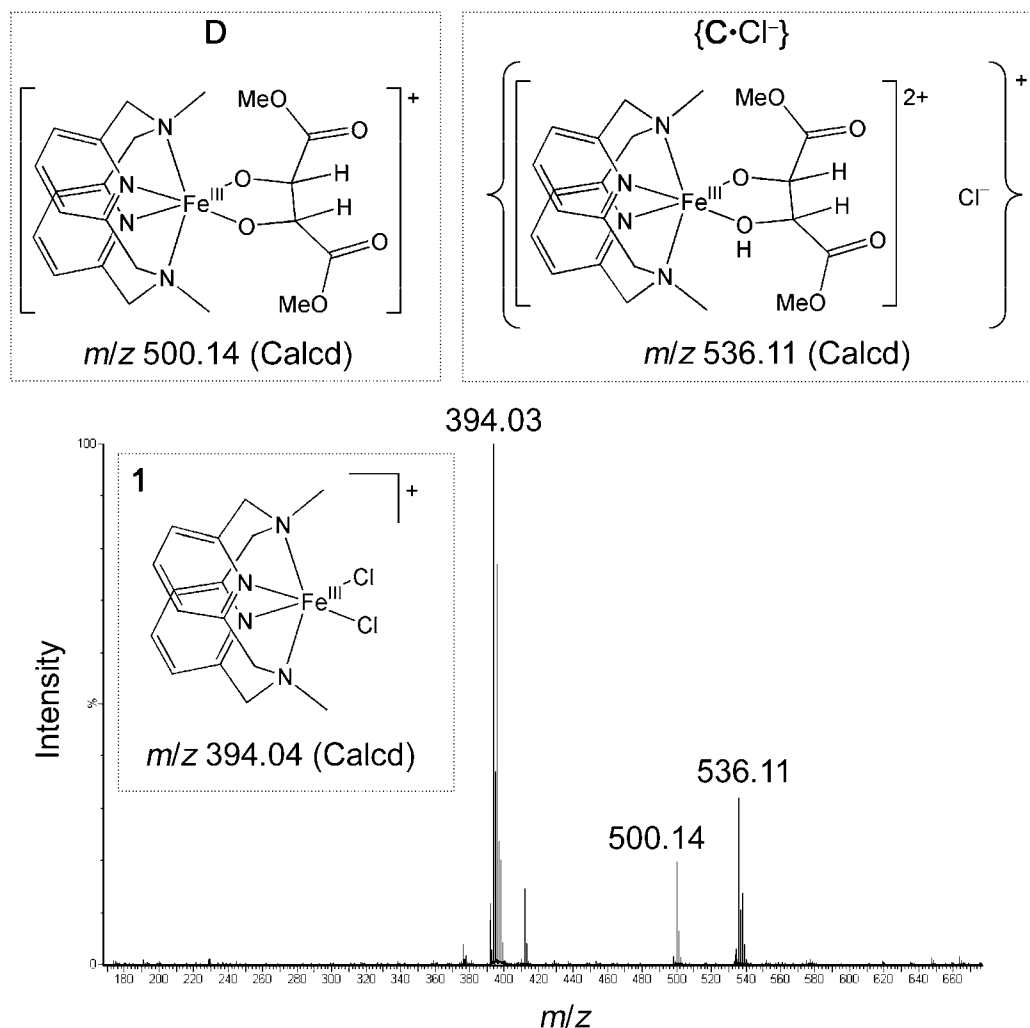


Figure 1. ESI mass spectrum of a reaction mixture of **1**, oxone (16 equiv), and dimethyl fumarate (**3i**, 10 equiv) in MeCN/H₂O (5:1 v/v) at room temperature.

of iron(II) to iron(III) by oxone (note a recent report on the oxidation of iron(II) to iron(III) with oxone³⁰), similar to the preoxidation of iron(II) to iron(III) involved in the iron(II)-catalyzed *cis*-dihydroxylation with H₂O₂ reported by Que and co-workers.^{13a} However, the formation of *cis*-Fe^{IV}(OH)₂ species from “Fe(ClO₄)₂·4H₂O + L-N₄Me₂” and oxone could not be excluded but might be less favored, as the DFT calculations by Comba and co-workers revealed that *cis*-Fe^{IV}(OH)₂ species is generated from an Fe^{II}(H₂O₂) species by O–O bond homolysis of the coordinated H₂O₂.¹⁵

Two possible pathways for the *cis*-dihydroxylation with oxone catalyzed by **1** are depicted in Scheme 2, one of which features *cis*-HO–Fe^V=O intermediate **A** whereas the other involves *cis*-O=Fe^V=O intermediate **B**; both **A** and **B** might react with alkene to afford *cis*-diol **I**, via intermediates **C** and **D**, respectively.

To gain further insight into the mechanism of the **1**-catalyzed alkene *cis*-dihydroxylation with oxone, we have made attempts to detect the reaction intermediates by ESI-MS and performed isotope labeling studies. DFT calculations on the reaction pathways depicted in Scheme 2 have also been conducted. In all these studies, dimethyl fumarate (**3i**) was selected as the

substrate (unless otherwise indicated), as this alkene gave the best results in the **1**-catalyzed *cis*-dihydroxylation with oxone (see Table 3).

i. ESI-MS. Upon treatment of **1** with oxone (16 equiv) and dimethyl fumarate (10 equiv) in MeCN/H₂O (5:1 v/v) at room temperature for ~30 s, we examined the reaction mixture by ESI-MS. The spectrum (Figure 1) shows prominent cluster peaks at *m/z* 536.11 attributable to {C•Cl[−]} (Calcd *m/z* 536.11) and at *m/z* 500.14 attributable to **D** or [{C•Cl[−]} - HCl] (Calcd *m/z* 500.14), as well as an intense cluster peak at *m/z* 394.03 assigned to **1**. The observed isotope patterns for the three cluster peaks well match their calculated ones (see Figures S4–S6 in the Supporting Information). Collision-induced dissociation of the ion with *m/z* 536.11 resulted in the formation of the ion with *m/z* 500.14 (Figure S7 in the Supporting Information), suggesting a fragmentation of {C•Cl[−]} to **D**, apparently by loss of HCl. For the ion with *m/z* 500.14, collision-induced dissociation generated an ion with *m/z* 412.12, possibly due to C–C bond cleavage of the coordinated diolate ligand in **D** (Figures S8 and S9 in the Supporting Information). ESI-MS analysis of the reaction mixture of **1** with oxone (4 equiv) and cyclooctene (**2a**, 20 equiv) was also performed, revealing a cluster peak at *m/z* 466.21 attributable to **D** or [C•H⁺] (Calcd *m/z* 466.20) (Figure S10 in the Supporting Information). This species showed a shorter lifetime than that of the corresponding species in the

(31) (a) Lahaye, D.; Groves, J. T. *J. Inorg. Biochem.* **2007**, *101*, 1786. (b) Jin, N.; Ibrahim, M.; Spiro, T. G.; Groves, J. T. *J. Am. Chem. Soc.* **2007**, *129*, 12416.

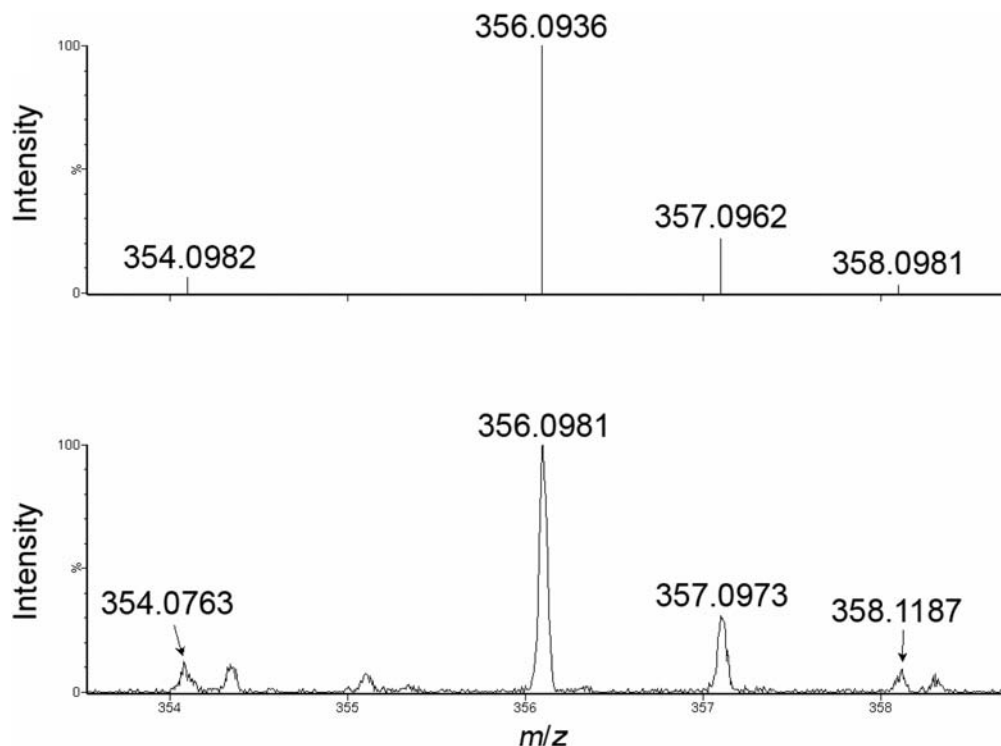


Figure 2. Upper: simulated isotope pattern for species **B**. Lower: observed isotope pattern in high-resolution ESI mass spectrum for the cluster peak at m/z 356.09 observed by ESI-MS analysis of a reaction mixture of $[\text{Fe}(\text{L-N}_4\text{Me}_2)\text{Br}_2]^+$ with oxone (8 equiv) in MeCN/H₂O (5:1 v/v) at room temperature.

reaction of **3i**, and was partially converted to **1** upon collision-induced dissociation (Figure S11 in the Supporting Information).

Efforts were also made to detect, by ESI-MS, oxoiron(V) species **A** and/or **B** (Scheme 2) using a reaction mixture of **1** with oxone in the absence of alkene substrate. As **B** has a calculated m/z value of 356.09, which is too close to the m/z 359.07 of the major fragment generated by collision-induced dissociation of **1** (Figure S12 in the Supporting Information), we changed the iron complex from **1** to $[\text{Fe}^{\text{III}}(\text{L-N}_4\text{Me}_2)\text{Br}_2]^+$ to avoid any overlap of the cluster peak of **B** with that of the major fragment of **1**. Importantly, analysis of a reaction mixture of $[\text{Fe}(\text{L-N}_4\text{Me}_2)\text{Br}_2]^+$ with oxone (8 equiv) in MeCN/H₂O (5:1 v/v) at room temperature by ESI-MS revealed a weak cluster peak at m/z 356.09 with an isotope pattern largely matching that simulated for **B** having a $[\text{Fe}(\text{L-N}_4\text{Me}_2)\text{O}_2]^+$ formulation (Figure 2). We assign this cluster peak to intermediate **B**, as no cluster peak ascribable to **A** (Calcd m/z 178.55) or $\{\text{A}\cdot\text{Br}^-\}$ (Calcd m/z 436.02) was found. However, the possible formation of **B** from **A** upon loss of H^+ under mass spectrometric conditions could not be excluded.

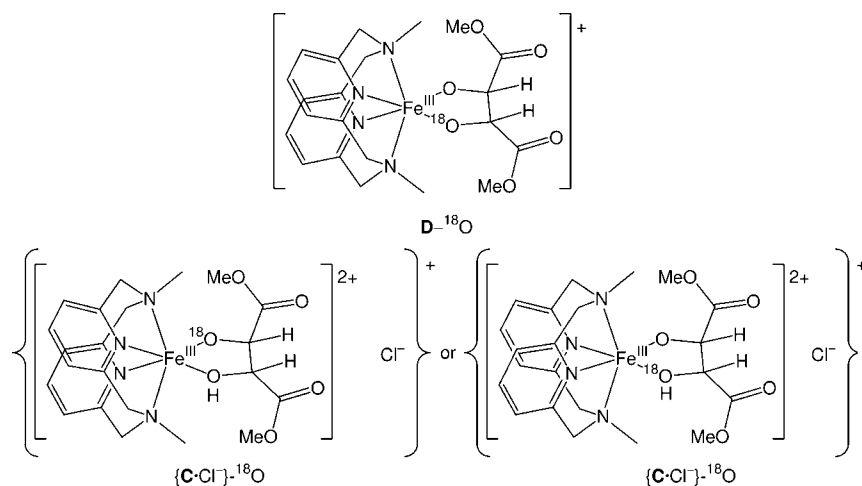
When H_2O_2 , instead of oxone, was employed to oxidize **2a** in the presence of catalyst **1** under similar conditions, ESI-MS analysis of the reaction mixture did not reveal cluster peaks ascribable to intermediate **C** or **D**. Such is also the case if $[\text{Fe}^{\text{III}}(\text{L-N}_4\text{H}_2)\text{Cl}_2]^+$, rather than **1**, was used as catalyst, irrespective of whether oxone or H_2O_2 was used as oxidant. In the ESI mass spectrum of the reaction mixture of $[\text{Fe}(\text{L-N}_4\text{Me}_2)\text{Br}_2]^+$ with H_2O_2 , there was no cluster peak ascribable to intermediate **A** or **B**. These may rationalize the ineffective *cis*-dihydroxylation of **2a** involving H_2O_2 or $[\text{Fe}^{\text{III}}(\text{L-N}_4\text{H}_2)\text{Cl}_2]^+$ performed in this work (Table 1).³² The higher activity of oxone relative to H_2O_2 in the **1**-catalyzed *cis*-dihydroxylation is reminiscent of a similar phenomenon previously reported by Meunier and co-workers^{29a} on the oxidation of lignin model compounds with oxone or H_2O_2 catalyzed by iron and manga-

nese porphyrins, which is considered to stem from highly favored heterolytic O–O bond cleavage of oxone, compared with H_2O_2 , for generation of high-valent metal-oxo intermediates, owing to more unsymmetrical O–O bond in oxone, together with SO_4^{2-} being a better leaving group than OH^- .^{29a}

ii. Isotope Labeling Studies. We analyzed the reaction mixture of **1** with oxone (16 equiv) and dimethyl fumarate (10 equiv) in MeCN/H₂¹⁸O (5:1 v/v) at room temperature in the presence of H_2^{18}O (~485 equiv). ESI-MS measurements suggested ~16% of ¹⁸O incorporation into **D** to form singly labeled species **D**-¹⁸O and ~10% of ¹⁸O incorporation into $\{\text{C}\cdot\text{Cl}^-\}$ to form singly labeled species $\{\text{C}\cdot\text{Cl}^-\}$ -¹⁸O (Chart 2; no doubly ¹⁸O labeled species were detected); these values of ¹⁸O incorporation were ~41% and ~38%, respectively, for the reaction of **1** with 2 equiv of oxone under the same conditions. When mixtures of H_2^{18}O and H_2^{16}O containing different amounts of H_2^{16}O were used, the ¹⁸O incorporation decreased with increasing content of H_2^{16}O . Therefore, the **1**-catalyzed *cis*-dihydroxylation of

(32) A facile oxidation (by oxone) of the secondary amine NH groups in the L-N₄H₂ ligand of $[\text{Fe}^{\text{III}}(\text{L-N}_4\text{H}_2)\text{Cl}_2]^+$, as mentioned in an earlier section, would significantly change the binding behavior of this macrocyclic ligand and hampers formation of the intermediates corresponding to **A**–**D** in Scheme 2. Indeed, in contrast to the easy recovery of L-N₄Me₂ at the end of **1**-catalyzed oxidation with oxone, neither L-N₄H₂ nor its iron complex was recovered after the corresponding catalysis using $[\text{Fe}^{\text{III}}(\text{L-N}_4\text{H}_2)\text{Cl}_2]^+$. For the **1**-catalyzed oxidation using H_2O_2 , the two coordinated Cl^- ligand in the starting catalyst might have a deleterious effect (see ref 17b) toward the *cis*-dihydroxylation (note that oxone can oxidize Cl^- , see: Dieter, R. K.; Nice, L. E.; Velu, S. E. *Tetrahedron Lett.* **1996**, *37*, 2377. Therefore, “ $\text{Fe}(\text{ClO}_4)_2\cdot 4\text{H}_2\text{O} + \text{L-N}_4\text{Me}_2$ ” (3.5 mol% each) were employed to catalyze the reaction of **2a** with H_2O_2 (4 equiv) in MeCN/H₂O (5:1 v/v) at room temperature for 1 h, which gave a 73% substrate conversion and a 74% mass balance (both substantially higher than those obtained for catalyst **1** (entry 8, Table 1)) but still afforded epoxide **II** as the major product (49% yield based on consumed substrate), with *cis*-diol **I** and α -hydroxy ketone **III** formed in 9% and 16% yields, respectively.

Chart 2



dimethyl fumarate (**3i**) with oxone is considerably assisted by water, providing evidence for the involvement of reaction 1 depicted in Scheme 2.

In previously reported isotope labeling studies on iron-catalyzed *cis*-dihydroxylation with H_2O_2 involving water-assisted mechanism, the extent of ^{18}O incorporation from $H_2^{18}O$ into the *cis*-diol products (singly labeled) is typically 60–97%;^{8d,9,11,13a,c,d} lower values of 33% and 29% were observed by Que,^{8e} Feringa,⁹ and co-workers, respectively, in some cases, which can be rationalized by water incorporation via nonwater-assisted pathway^{8e} or by the likely existence of several competing pathways.⁹ The up to ~41% ^{18}O incorporation observed for the **1**-catalyzed *cis*-dihydroxylation with oxone is indicative of the involvement of both reactions 1 and 2 (Scheme 2) in this catalytic process.

In addition, we examined a reaction of **1** (0.1 mmol) with oxone (1 equiv) and **3a** (1 equiv) in MeCN/ H_2O (2 mL each) at room temperature for 5 min, which gave the *cis*-diol **I** in 55% yield (determined by 1H NMR; substrate conversion: 100%), considerably lower than the 81% yield obtained under the catalytic conditions. This may imply that more than one equivalent of oxone is needed to convert **1** to the reactive oxoiron(V) species in these oxidation processes and is supportive of both reactions 1 and 2 depicted in Scheme 2.

iii. DFT Calculations. There have been extensive theoretical studies, such as DFT calculations, on the mechanism of alkene *cis*-dihydroxylation catalyzed by OsO_4 ,³³ which generally favor a concerted [3 + 2] cycloaddition mechanism. A concerted [3 + 2] cycloaddition mechanism is also favored for the reaction of RuO_4 with ethene on the basis of DFT calculations by Frenking and co-workers,³⁴ and for the alkene *cis*-dihydroxylation by *cis*- $[Ru^{VI}(Me_3tacn)O_2(OCOFCF_3)]^+$ according to our

previous experimental investigations.¹⁹ DFT calculations on the mechanisms of iron-catalyzed analogues are sparse,^{16d,15} revealing *cis*-dihydroxylation of alkenes (such as 2-butene) by *cis*-HO- $Fe^V=O$ species via an oxoiron-containing carbon radical (which is converted to the cycloadduct without any significant energy barrier) as reported by Que and co-workers,^{16d} and the concerted *cis*-dihydroxylation of ethene by *cis*- $Fe^{IV}(OH)_2$ species as reported by Comba and co-workers.¹⁵

In this work, the mechanisms of *cis*-dihydroxylation of dimethyl fumarate (**3i**) by oxoiron(V) species **A** and **B** (Scheme 2) were investigated with hybrid density functional theory at the B3LYP/6-31G(d):lanl2dz for Fe level. Before exploring the potential energy surface of the reactions, we conducted computational studies on the relative energy of the separated reactants “**3i** + **A**” and “**3i** + **B**” and the respective products **C** and **D** (Scheme 2) with different spin multiplicities. The calculated results reveal that the ground states of **A** and **B** feature quartet Fe^V centers; this spin state was considered in subsequent calculations. The computed structure and conformation of the $L-N_4Me_2$ ligand in **A** and **B** are consistent with those of $L-N_4Me_2$ in the crystal structures of **1**· $FeCl_4$ and **1**· ClO_4 ·MeCN, and the computed $Fe^V=O$ distances (1.613–1.638 Å) in **A** and **B** (Figure S13 in the Supporting Information) are similar to those computed for the bent $[O=Fe^V=O]^+$ (1.63–1.70 Å),²¹ the *cis*-HO- $Fe^V=O$ species $[Fe^V(TPA)(O)(OH)]^{2+}$ (1.66 Å, TPA = tris(2-pyridylmethyl)amine)^{16a} and the oxoiron(V) complex $[Fe^V(TAML)(O)]^-$ (1.60 Å, H_4TAML = a macrocyclic tetraamide).³⁵

The reaction of **3i** with **A** was found to involve initial formation of a σ -complex **CP1**, which is then converted to a radical intermediate **CP2** via transition state **TS**,³⁶ followed by conversion of **CP2** to cycloadduct **C** (Figure 3, upper). Similarly, the reaction of **3i** with **B** (Figure 3, lower) starts with a σ -complex **CP1'**, with subsequent formation of a radical intermediate **CP2'** via transition state **TS'**, followed by formation of cycloadduct **D**. The calculated structures, along with key bond

(33) (a) Pidun, U.; Boehme, C.; Frenking, G. *Angew. Chem., Int. Ed. Engl.* **1996**, *35*, 2817. (b) Dapprich, S.; Ujaque, G.; Maseras, F.; Lledós, A.; Musaev, D. G.; Morokuma, K. *J. Am. Chem. Soc.* **1996**, *118*, 11660. (c) Torrent, M.; Deng, L.; Duran, M.; Sola, M.; Ziegler, T. *Organometallics* **1997**, *16*, 13. (d) DelMonte, A. J.; Haller, J.; Houk, K. N.; Sharpless, K. B.; Singleton, D. A.; Strassner, T.; Thomas, A. A. *J. Am. Chem. Soc.* **1997**, *119*, 9907. (e) Ujaque, G.; Maseras, F.; Lledós, A. *J. Am. Chem. Soc.* **1999**, *121*, 1317. (f) Norrby, P.-O.; Rasmussen, T.; Haller, J.; Strassner, T.; Houk, K. N. *J. Am. Chem. Soc.* **1999**, *121*, 10186. (g) Frstrup, P.; Tanner, D.; Norrby, P.-O. *Chirality* **2003**, *15*, 360. (h) Ujaque, G.; Maseras, F.; Lledós, A. *Eur. J. Org. Chem.* **2003**, 833.

(34) Frunzke, J.; Loschen, C.; Frenking, G. *J. Am. Chem. Soc.* **2004**, *126*, 3642.

(35) Tiago de Oliveira, F.; Chanda, A.; Banerjee, D.; Shan, X.; Mondal, S.; Que, L., Jr.; Bominaar, E. L.; Münck, E.; Collins, T. J. *Science* **2007**, *315*, 835.

(36) In the conversion of **CP1** to **CP2** via **TS**, the alkene group of **3i** is attacked mainly by the oxo group of intermediate **A**. An alternative pathway is the initial attack of the alkene group mainly by the hydroxo group of **A**, but this pathway was found to have a higher barrier (for more detail, see Figure S15 in the Supporting Information).

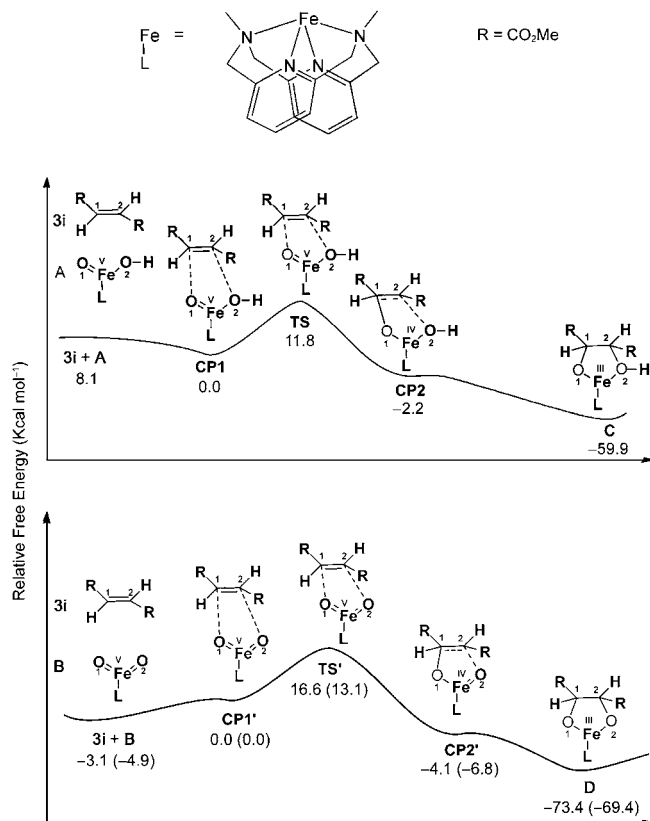


Figure 3. Relative free energy profiles in gas phase and selected parameters of stationary points for the reactions of dimethyl fumarate (**3i**) with oxoiron(V) species **A** (upper) and **B** (lower). The free energies of activation (ΔG_{solv} in kcal mol⁻¹) in MeCN solvent at CPCM(bondi)-B3LYP/6-31G(d):lanl2dz for Fe level of theory are in the parentheses.

distances, are depicted in Figure 4 for **TS**, **C**, **TS'**, and **D**, and in Figure S13 (see the Supporting Information) for **CP1**, **CP2**, **CP1'**, and **CP2'**.³⁷

Both the mechanisms involving **A** and **B** have an asymmetric transition state (**TS** or **TS'**), in which the C(1)–O(1) distance is significantly shorter than that in the σ -complex (1.931 vs 2.896 Å for **TS** vs **CP1**, 1.974 vs 2.865 Å for **TS'** vs **CP1'**). Also, the iron center changes its oxidation state from Fe^V to Fe^{IV} upon conversion of the σ -complex (**CP1** or **CP1'**) to the radical intermediate (**CP2** or **CP2'**), and from Fe^{IV} to Fe^{III} in subsequent conversion of the radical intermediate to the cycloadduct (**C** or **D**). All these conversions are exothermic processes.

However, compared with the reaction of **3i** with **A**, the reaction of the same alkene with **B** shows several differences: (i) In terms of relative energy (ΔE), the σ -complex (**CP1'**) is more stable than the separate reactants (**3i** + **B**) by 7.2 kcal mol⁻¹, a value smaller than that of 19.0 kcal mol⁻¹ (**CP1** vs “**3i** + **A**”) in the reaction with **A**. (ii) The relative free energy (ΔG) of **CP1'** is 3.1 kcal mol⁻¹ higher than that of “**3i** + **B**”;

(37) Concerning the conversions of **CP2** → **C** and **CP2'** → **D**, one transition state (**TS2**) was located on quartet state in the former case (no transition state was successfully located for the latter conversion at the B3LYP/6-31G(d):lanl2dz level of theory). However, the transition state **TS2** was found to be heavily contaminated by other spin states ($\langle S^2 \rangle = 4.63$), rendering it hard to obtain an accurate energy of **TS2** by the theoretical method (B3LYP) employed in our study (the calculated free energy of **TS2** is lower by 4.2 kcal/mol than that of **CP2** due to the underestimation of **TS2** energy resulting from spin contamination). For this reason, **TS2** is not shown in Figure 3. The calculated structure of this transition state is depicted in Figure S14 in the Supporting Information.

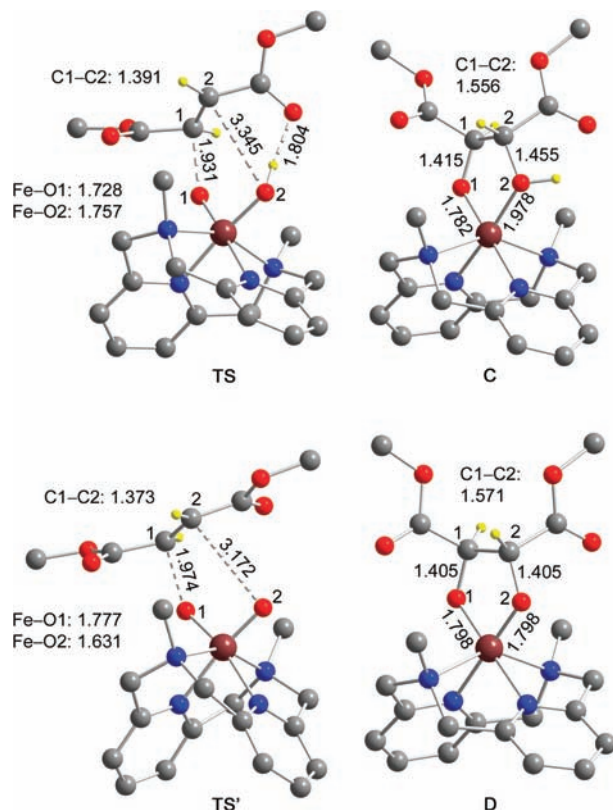


Figure 4. Calculated structures of transition states **TS** and **TS'** and cycloadducts **C** and **D** with omission of hydrogen atoms except those bonded to C1, C2, and O2 atoms. The key bond distances (Å) are indicated.

on the contrary, **CP1** has a ΔG value lower than that of “**3i** + **A**” by 8.1 kcal mol⁻¹. (iii) The structure of **CP1'** has identical C(1)–O(1) and C(2)–O(2) distances (2.865 Å), whereas different C(1)–O(1) and C(2)–O(2) distances (2.896 and 3.853 Å, respectively) are found in **CP1**. (iv) On going from **CP1'** to **TS'**, the C(2)–O(2) distance increases from 2.865 to 3.172 Å, unlike a decrease of C(2)–O(2) distance from 3.853 to 3.345 Å on going from **CP1** to **TS**. (v) The transition state **TS'** has a higher free energy of activation (16.6 kcal mol⁻¹) than that (11.8 kcal mol⁻¹) for the transition state **TS** (Figure 3).

As MeCN was used as a solvent in the **1**-catalyzed *cis*-dihydroxylation of **3i**, the solvation effect on the reaction energetics for the oxidation of **3i** by **B** was examined by SCRFF calculations (CPCM) using the gas-phase geometry with MeCN as the solvent. The results of bulk effect show that the barrier of the first oxidation step decreases from 16.6 (ΔG_{gas}) to 13.1 (ΔG_{solv}) kcal mol⁻¹ (Figure 3, the data in parentheses). From the value (13.1 kcal mol⁻¹) of the free energy of activation in the rate-determining conversion of the σ -complex **CP1'** to the radical intermediate **CP2'**, one can roughly estimate that the half lifetime of the reactants is on the scale of 10⁻³ s according to the transition state theory and by supposing the reaction is of first-order. Therefore, the present computational results suggest that a *cis*-dioxoiron(V) species could be a reaction intermediate for direct *cis*-dihydroxylation of alkenes.

On the basis of above ESI-MS, isotope labeling studies, and DFT calculations, we propose that the **1**-catalyzed *cis*-dihydroxylation of alkenes with oxone could involve *cis*-HO–Fe^V=O and/or *cis*-O=Fe^V=O intermediates, as the *cis*-dioxoiron(V) species results in a reasonable barrier (16.6 kcal mol⁻¹), although this larger barrier than that for *cis*-HO–Fe^V=O (11.8 kcal mol⁻¹) would render the *cis*-dihydroxylation by *cis*-

$\text{O}=\text{Fe}^{\text{V}}=\text{O}$ a less favorable pathway. We note that a related structurally characterized $\text{cis-O}=\text{Ru}^{\text{V}}=\text{O}$ complex, $\text{cis-}[\text{Ru}^{\text{V}}\text{LO}_2]^+$ ($L = N,N,N',N',3,6\text{-hexamethyl-3,6-diazaoctane-1,8-diamine}$), is stable toward protonation at $\text{pH} \geq 3.0$; thus it is not unreasonable to conceive that the $\text{cis-O}=\text{Fe}^{\text{V}}=\text{O}$ species **B** is the major oxoiron(V) species present in the solution under the catalytic conditions ($\text{pH} 7$).³⁸ The reaction of $\text{cis-HO-Fe}^{\text{V}}=\text{O}$ and $\text{cis-O}=\text{Fe}^{\text{V}}=\text{O}$ intermediates with alkene to give cycloadducts **C** and **D** via **CP2** and **CP2'**, respectively, has no significant activation barrier in the conversion of **CP2/CP2'** to **C/D**, and therefore can be described as a concerted but highly asynchronous process, in which the formation of the second C–O bond is coupled to the formation of the first one. This concerted mechanism revealed by DFT calculations is consistent with the absence of appreciable *trans*-diol product in the catalytic reactions.

Conclusion

By using iron complexes of a macrocyclic tetraaza ligand, we have developed an efficient and selective metal-catalyzed *cis*-dihydroxylation of alkenes with oxone as terminal oxidant. This iron-catalyzed reaction proceeds rapidly at room temperature, uses limiting amounts of alkene substrates, and can be performed on ~ 10 g scale, providing a convenient protocol for practical *cis*-dihydroxylation of electron-deficient alkenes (such as α,β -unsaturated esters). High-valent oxoiron(V) species $\text{cis-HO-Fe}^{\text{V}}=\text{O}$ and/or $\text{cis-O}=\text{Fe}^{\text{V}}=\text{O}$ might be involved in the alkene *cis*-dihydroxylation with oxone catalyzed by $[\text{Fe}^{\text{III}}(\text{L-N}_4\text{Me}_2)\text{Cl}_2]^+$ (**1**). According to DFT calculations, the *cis*-dihydroxylation reactions by $\text{cis-HO-Fe}^{\text{V}}=\text{O}$ and $\text{cis-O}=\text{Fe}^{\text{V}}=\text{O}$ both occur by a concerted but highly asynchronous pathway, with the *cis*-dioxoiron(V) species resulting in a larger activation barrier. Taking also into account the [3 + 2] cycloaddition of *cis*-dioxoruthenium complexes with alkenes, it is apparent that reactive *cis*-dioxometal species other than that of osmium could be harnessed for alkene *cis*-dihydroxylation.

Experimental Section

General. Oxone and NaHCO_3 (purchased from Sigma-Aldrich) were used as received. Alkene substrates **2a–h** and **3a–j** were purified by column chromatography on silica gel or Al_2O_3 . Complexes $[\text{Fe}^{\text{III}}(\text{Me}_3\text{tacn})\text{Cl}_3]$ ³⁹ and $[\text{Fe}^{\text{III}}(\text{L-N}_4\text{H}_2)\text{Cl}_2]^+$ ²⁷ were prepared as described in the literature. $[\text{Fe}^{\text{II}}(\text{qpy})\text{Cl}_2]$ and $[\text{Fe}^{\text{II}}(6\text{-Me}_2\text{-bpmcn})\text{Cl}_2]$ were prepared according to the same procedures as those reported for $[\text{Fe}^{\text{II}}(\text{qpy})(\text{MeCN})_2](\text{ClO}_4)_2$ ⁴⁰ and $[\text{Fe}^{\text{II}}(\text{bpmcn})\text{Cl}_2]$,⁴¹ respectively, except that FeCl_2 (instead of $\text{Fe}(\text{ClO}_4)_2$) was used in the former case and 6-Me₂-bpmcn (instead of bpmcn) was used in the latter case. Catalysts $[\text{Fe}^{\text{III}}(\text{L-N}_4\text{Me}_2)\text{Cl}_2]^+$ (**1**) and $[\text{Fe}^{\text{III}}(\text{L-N}_4\text{Me}_2)\text{Br}_2]^+$ were prepared from reactions of L-N₄Me₂ with $\text{FeCl}_3 \cdot 6\text{H}_2\text{O}$ and FeBr_3 , respectively (see the Supporting Information for detailed procedures).

General Procedure for *cis*-Dihydroxylation of Alkenes with Oxone Catalyzed by **1.** A solution of oxone (1.0 mmol) and NaHCO_3 (3.0 mmol) in water (6 mL) was added in two portions

to a solution of alkene (0.5 mmol) and **1** (0.7–3.5 mol %) in acetonitrile (6 mL) at room temperature within 5 min. Upon quenching by aqueous saturated Na_2SO_3 solution, the mixture was extracted with ethyl acetate (10 mL) containing 1,4-dichlorobenzene (GC internal standard, 0.1 mmol). An aliquot of the extract was analyzed by GC. Afterward, the mixture was further extracted with ethyl acetate (3×50 mL). The organic products (diol and α -hydroxy ketone) were identified and quantified by ¹H NMR analysis, or isolated after purification by column chromatography on silica gel.

Large-Scale *cis*-Dihydroxylation of Methyl Cinnamate (3a**) with Oxone Catalyzed by **1**.** A solution of oxone (30 mmol) and NaHCO_3 (90 mmol) in water (300 mL) was added in two portions to a solution of methyl cinnamate (30 mmol) and **1** (1.4 mol %) in acetonitrile (300 mL) at room temperature within 5 min. To the reaction mixture was added a solution of methyl cinnamate (30 mmol) and $\text{Fe}(\text{ClO}_4)_2 \cdot 4\text{H}_2\text{O}$ (1.4 mol %) in acetonitrile (300 mL), followed by addition of a solution of oxone (30 mmol) and NaHCO_3 (90 mmol) in water (300 mL) in the same manner as described above. After quenching by aqueous saturated Na_2SO_3 solution, the reaction mixture was extracted with ethyl acetate (4×500 mL), and the extract was subjected to GC and ¹H NMR analysis for product identification and quantification. The *cis*-diol product was isolated after purification by column chromatography on silica gel.

Reuse of L-N₄Me₂ Ligand in Iron-Catalyzed *cis*-Dihydroxylation of Methyl Cinnamate (3a**) with Oxone.** A solution of oxone (1.0 mmol) and NaHCO_3 (3.0 mmol) in water (6 mL) was added in two portions to a solution of methyl cinnamate (0.5 mmol) and **1** (1.4 mol %) in acetonitrile (6 mL) at room temperature within 5 min. Subsequent runs were performed by adding a solution of methyl cinnamate (0.5 mmol) and $\text{Fe}(\text{ClO}_4)_2 \cdot 4\text{H}_2\text{O}$ (1.4 mol %) in acetonitrile (6 mL) to the reaction mixture followed by addition of a solution of oxone (1.0 mmol) and NaHCO_3 (3.0 mmol) in water (6 mL) in the same manner as described above. The reaction was quenched by saturated aqueous Na_2SO_3 solution after all desired runs were completed. The reaction mixture was extracted with ethyl acetate (3×100 mL), and the extract was subjected to GC and ¹H NMR analysis for product identification and quantification.

Computational Details. B3LYP/6-31G(d):lanl2dz for Fe density functional theory method was employed to optimize local minima on the potential energy hypersurfaces corresponding to the reactant complex, the reaction intermediates, the final complex, and other fragment species. Vibrational analyses were systematically carried out to ensure that the optimized geometries correspond either to a local minimum that has no imaginary frequency mode or to a saddle point that has only one imaginary frequency mode. Cartesian coordinates for stationary structures are included in the Supporting Information (Table S4). The bulk effect on the dihydroxylation of alkene by *cis*-dioxoiron(V) species **B** was investigated by the SCRF calculation using CPCM-bondi model at the B3LYP/6-31G(d):lanl2dz for Fe level of theory.

Acknowledgment. This work was supported by The University of Hong Kong (University Development Fund), the University Grants Council of HKSAR (the Area of Excellence Scheme: AoE 10/01P), and the Hong Kong Research Grants Council (HKU 1/CRF/08, HKU 7007/08P). We are grateful to Dr. Nianyong Zhu for assistance in solving the X-ray crystal structures of **1**· FeCl_4 and **1**· ClO_4 ·MeCN.

Supporting Information Available: Physical measurements, procedures for catalyst preparation and product characterization, Tables S1–S4, Scheme S1, Figures S1–S15, and CIF files for the crystal structures of **1**· FeCl_4 and **1**· ClO_4 ·MeCN. This material is available free of charge via the Internet at <http://pubs.acs.org>.

JA100967G

(38) We examined the pH dependence of the **1**-catalyzed *cis*-dihydroxylation of **2e** with oxone (by adjusting the amount of NaHCO_3 used in the reaction). Upon increasing pH from 7 to 8–9, a decrease in the efficiency of *cis*-dihydroxylation was found (substrate conversion: from 89% to 60%, yield of *cis*-diol **I**: from 44% to 25%, yield of epoxide: from 19% to 22%). We noted that **1** became significantly less stable at pH 8–9.

(39) Chaudhuri, P.; Winter, M.; Wieghardt, K.; Gehring, S.; Haase, W.; Nuber, B.; Weiss, J. *Inorg. Chem.* **1988**, *27*, 1564.

(40) Wong, E. L.-M.; Fang, G.-S.; Che, C.-M.; Zhu, N. *Chem. Commun.* **2005**, 4578.

(41) Costas, M.; Que, L., Jr. *Angew. Chem., Int. Ed.* **2002**, *41*, 2179.